The International Journal of Biochemistry & Cell Biology 84 (2017) 89–95

Contents lists available at ScienceDirect

The International Journal of Biochemistry & Cell Biology

journal homepage: www.elsevier.com/locate/biocel

Imaging in focus

Characterising live cell behaviour: Traditional label-free and quantitative phase imaging approaches

Richard Kasprowicz[a,b,*], Rakesh Suman[a,b], Peter O'Toole[b,*]

[a] Phasefocus Ltd, Sheffield, UK
[b] Technology Facility, University of York, UK

ARTICLE INFO

Article history:
Received 15 September 2016
Received in revised form
23 December 2016
Accepted 6 January 2017
Available online 20 January 2017

Keywords:
Ptychography
Label-free imaging
QPI
Quantitative phase imaging
Live-cell imaging

ABSTRACT

Label-free imaging uses inherent contrast mechanisms within cells to create image contrast without introducing dyes/labels, which may confound results. Quantitative phase imaging is label-free and offers higher content and contrast compared to traditional techniques. High-contrast images facilitate generation of individual cell metrics *via* more robust segmentation and tracking, enabling formation of a label-free dynamic phenotype describing cell-to-cell heterogeneity and temporal changes. Compared to population-level averages, individual cell-level dynamic phenotypes have greater power to differentiate between cellular responses to treatments, which has clinical relevance *e.g.* in the treatment of cancer. Furthermore, as the data is obtained label-free, the same cells can be used for further assays or expansion, of potential benefit for the fields of regenerative and personalised medicine.

1. Introduction: the need for label-free imaging

Label-free imaging ensures that native cell behaviour remains uninfluenced by the recording process. In this mini-review, we focus on differences between quantitative phase imaging (QPI) and traditional label-free imaging techniques regarding: (i) the importance of image contrast for enabling robust, automated extraction of metrics describing individual cell behaviour; (ii) the power of a label-free dynamic phenotype over global population-level measurements in identifying changes in cell behaviour.

1.1. Visualising cells and contrast-enhancing agents

Cells are phase objects, *i.e.* absorb little light, resulting in only minor changes in the amplitude of transmitted light through the cell. Since the human eye relies on changes in amplitude of a light wave, cells can be difficult to visualise using a light microscope without a system to enhance cell contrast. One widespread solution is to introduce dyes/labels; these provide molecular specificity but can involve procedures (*e.g.* fixation) incompatible with live cell imaging. Even labels designed for use with live cell imaging can cause perturbation to normal cellular function and concentration-dependent toxicity effects (Alford et al., 2009; Coutu and Schroeder, 2013).

1.2. Phototoxicity

Phototoxicity poses additional barriers to imaging native cell behaviour, as the light intensity required to excite a fluorophore can cause cells to behave abnormally or die (Mov. 1). Phototoxicity is primarily attributed to generation of reactive oxygen species, which adversely affect cell physiology, health, behaviour, movement and shape by various mechanisms (Magidson and Khodjakov, 2013). Subtler phototoxic effects can easily be overlooked, confounding experimental results (Saetzler et al., 1997; Tinevez et al., 2012), and are further exacerbated when imaging over extended periods, *e.g.* causing impairment of cell doubling time (Carlton et al., 2010). The impact of phototoxic damage can be assessed and limited but not negated (Magidson and Khodjakov, 2013; Tinevez et al., 2012). Thus, imaging under very low light intensity without labels is an attractive solution to enhance cell contrast whilst minimising uncertainty in the recording of native cell behaviour. Furthermore, label-free techniques enable researchers to avoid the cost of time-intensive dye/label optimisation or stable fluorescent-reporter cell line generation.

* Corresponding author at: Technology Facility, Department of Biology, University of York, UK.
E-mail addresses: richard.kasprowicz@york.ac.uk (R. Kasprowicz), peter.otoole@york.ac.uk (P. O'Toole).

http://dx.doi.org/10.1016/j.biocel.2017.01.004

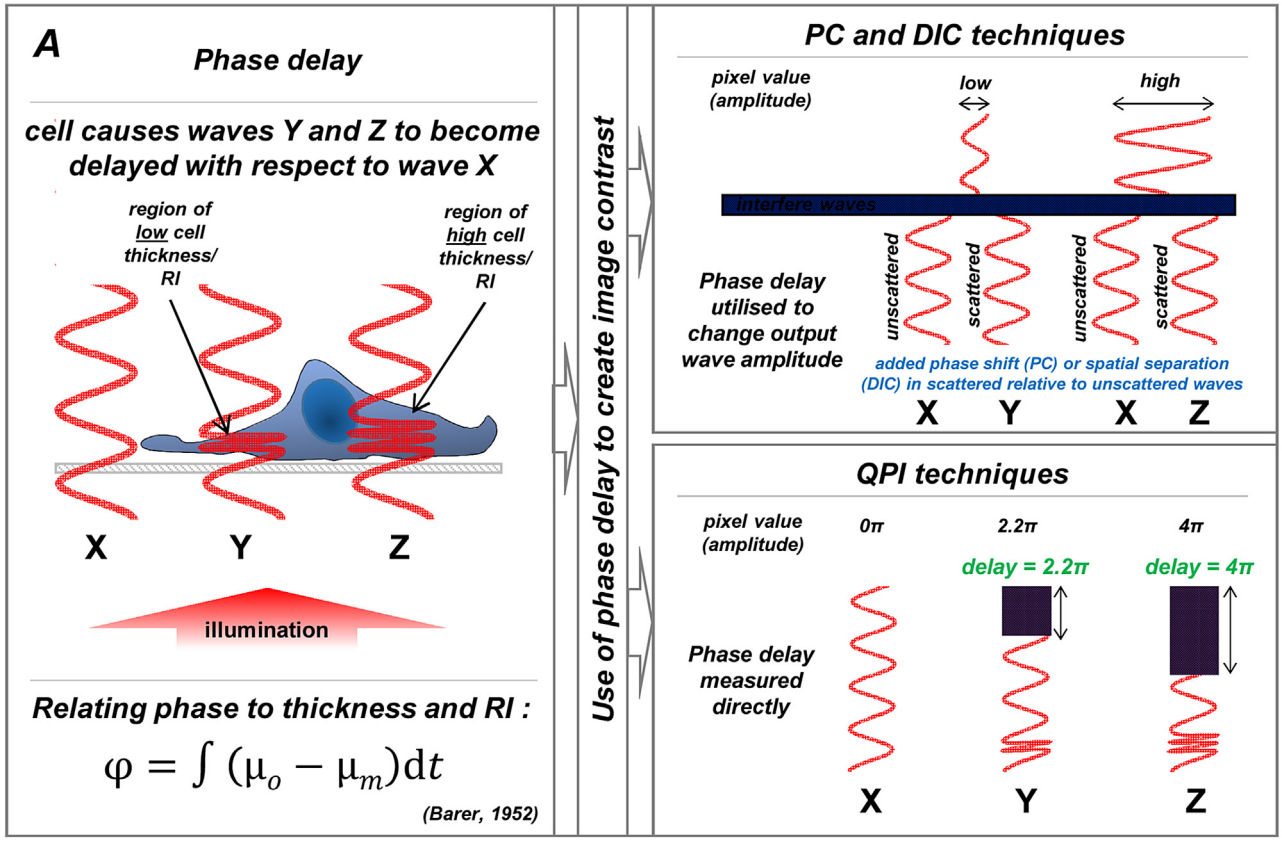

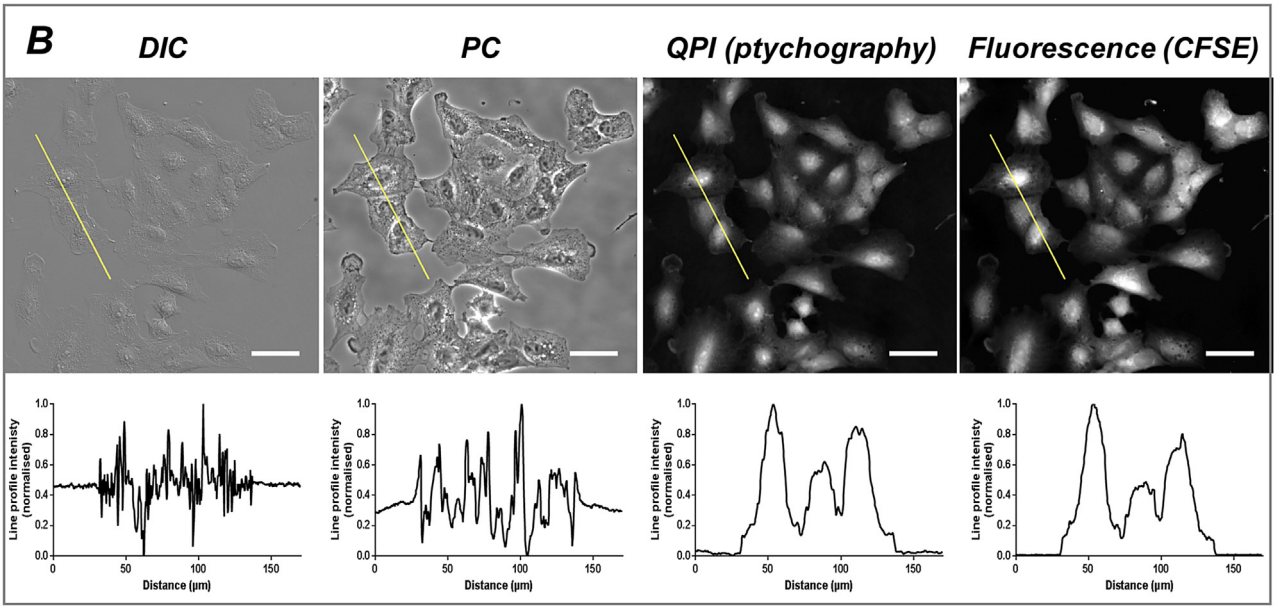

Fig. 1. High-contrast images are obtained by QPI techniques. (A) Diagram of phase delay caused by a cell and the basis by which the phase delay is used to create contrast in the image. The equation describes how phase delay (φ) is calculated from thickness (t) and the difference in refractive index (RI) of the object (μ_o) and media (μ_m). Whilst traditional techniques (PC, DIC) use the phase delay to alter the amplitude of the exit wave resulting in changes in pixel intensity, in quantitative techniques (QPI) the phase delay is measured directly and is enumerated as a pixel intensity. (B) Line profiles across three adjacent A549 cells in an identical field of view imaged by DIC, PC, ptychographic QPI and whole-cell fluorescence. A549 cells were labelled with CFSE and fixed. Scale bar, 50 μm.

2. What are the label-free options?

Rather than requiring contrast-enhancing dyes/labels, label-free solutions rely on components of the optical setup that exploit cells' inherent contrast mechanisms (thickness and refractive index (RI)) to create image contrast.

2.1. Traditional techniques

Phase contrast (PC) and differential interference contrast (DIC) microscopy remain the most prevalent label-free imaging techniques in biological research. Both techniques employ specific optical setups that translate differences in phase caused by cells and intracellular features into changes in light wave amplitude.

Table 1
Examples of common metrics of a label free dynamic phenotype. n, refractive index; λ, illumination wavelength; a yields a range of values between 0 and 1, with a value of one being completely spherical/circular; b range of values between −90° to +90°.

Dynamic metrics	Morphological metrics	Unique phase metrics
Track Length total distance travelled by a cell (μm)	**Confluency (%)** *(area covered by cells/ area of imaged region) *100*	**Dry mass** *∑phase values per cell * λ * refractive increment*
Mean Speed *track length over time (μm/min)*	**Area** *cell footprint (μm^2)*	**Mean Thickness** *mean phase value per cell * $\lambda/(2*\pi*[n_{cell} - n_{media}])$*
Instantaneous Velocity *the velocity of a cell between successive frames (μm/s)*	**Perimeter** *Distance (μm) around the boundary of an object*	**Sphericity**[a] *(surface integral of phase + area of a cell) / surface area of a sphere with a volume equal to the integrated thickness of the cell*
Euclidian Distance *straight line distance to the track origin*	**Circularity**[a] *4π * (area/ perimeter^2)*	
Meandering Index *displacement from origin/ track length*	**Aspect Ratio**  *ratio of L:W of an ellipse fitted to the cell*	
Angular Velocity *rate of change of direction of travel between successive frames*	**Orientation**[b] 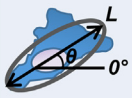 *angle (θ) of L compared to a horizontal axis of 0°*	**Phase skewness** *measures lack of symmetry in phase value from mean thickness*

Unlike changes in phase, these can be detected by the human eye or recorded as pixel intensity changes on a camera (Fig. 1a). However, the intensity in PC and DIC images is non-quantitative of the phase delay, and low image contrast can make automated image segmentation difficult at high cell densities.

2.2. Quantitative phase imaging

Quantitative phase imaging (QPI) is a label-free technique in which various methods (*e.g.* holography, ptychography) can be used to retrieve the phase information of light passing through the cell. QPI techniques quantify the extent of phase delay introduced by the sample and record it as pixel values within the generated image. Pixel intensity is dictated by physical thickness and the RI of the cell, the latter being a readout of biomolecule composition and organisation (Fig. 1a) (Barer, 1952; Zangle and Teitell, 2014). QPI produces high contrast images, with cells appearing as bright objects on a dark background (Fig. 1a) making automated cell segmentation simpler and more reliable. Commercially-available QPI systems can be broadly classified according to the phase retrieval method utilised: (i) off-axis digital holography (PhiAB, Nanolive, Lyncee Tec, Tescan,[1] Ovizio); (ii) wavefront sensing (Phasics); (iii) spatial light interference (Phi Optics); (iv) ptychography (Phasefocus).

3. Dynamic phenotype generation: from images to numbers

Automated segmentation, tracking and linage determination enables generation and study of the dynamic phenotype of cells. The type and quality of images acquired influence the success of cell segmentation (object identification and separation). Typical segmentation algorithms utilise a combination of feature detection, morphological filtering, region accumulation, deformable model fitting, and intensity thresholding processes (Meijering, 2012). Classical intensity thresholding and, increasingly, deformable models are the most widely used segmentation techniques within biological research (Bajcsy et al., 2015; Meijering, 2012).

3.1. QPI images are of higher contrast than PC and DIC images

QPI produces images of high contrast: intensity profiles illustrate that the highest concentration of a cell's mass is typically the point of peak intensity, boundaries between adjacent cells appear as intensity clefts, and the cells cause unidirectional changes in intensity with reference to a low intensity, flat background (Fig. 1b). These image properties make label-free QPI images appear fluorescence-like, sharing a similar-shaped intensity profile to that of a cell labelled with a whole-cell fluorescent dye (Fig. 1b). Therefore software packages (Wiesmann et al., 2015) and segmentation algorithms optimised for use with fluorescence images, in particular those developed using whole-cell fluorescence intensity images (Arce et al., 2013; Maska et al., 2013), can be utilised for segmentation of QPI images (Rappaz et al., 2014).

Compared to QPI, segmentation of PC and DIC images poses extra challenges because the intensity profiles are bidirectional, with peaks and troughs that neither clearly indicate the cell centre nor boundaries between adjacent cells (Fig. 1b) (Marrison et al., 2013; Rappaz et al., 2014). Although segmentation is possible (Nketia et al., 2014; Winter et al., 2011), these factors make individual cell segmentation of PC and DIC images notoriously difficult, especially at high densities. Obtaining individual cell data with PC/DIC images often requires correlative fluorescence imaging of nuclear labels *e.g.* H2B-GFP. Yet, such strategies can result in loss of morpholog-

[1] coherence-controlled.

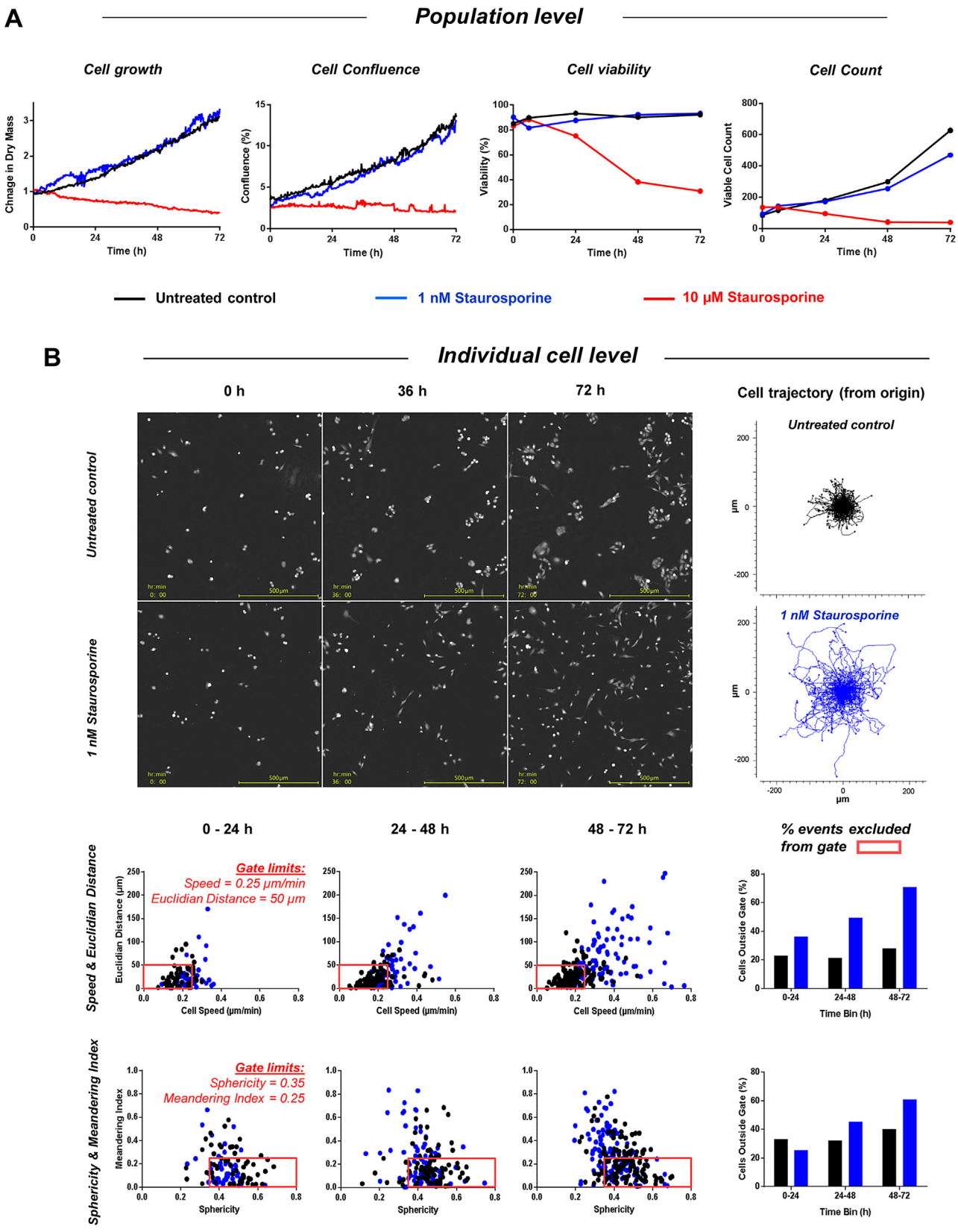

Fig. 2. Resolving between drug treatments using population-level and individual-cell metrics of a dynamic phenotype. (A) Population-level: Plots show the rate of change of dry mass, confluence, viability and viable cell count of the MDA-MB-231 cell population measured by ptychographic QPI (Livecyte, Phasefocus) and trypan blue exclusion (Vi-CELL, Beckman Coulter) upon treatment with 1 nM or 10 µM Staurosporine compared to untreated control over a 72 h period. (B) Individual-cell level: Images taken from the ptychographic QPI time-sequence (10X/0.25 objective; 72 h duration; 10 min imaging interval) indicate differences in dispersal of individual MDA-MB-231 cells between untreated controls and 1 nM Staurosporine treatment. Segmentation, tracking (Cell Analysis Toolbox, Phasefocus) and post-filtering (exclusion of events <200 µm2 and tracked for <6.7 h) enables the behaviour of individual cells to be quantified. Cell trajectory plots confirm that 1 nM Staurosporine causes increased cell dispersal compared to the untreated control. Dot plots show combinatorial metric analysis, with each point demarking the metric mean value for an individual cell over a 24 h time window.

ical data due to the difficulties of extrapolating the segmentation boundary from the nuclear label to the ill-defined cell boundary.

3.2. Accurate segmentation and tracking

Ideally, segmentation algorithms should be able to cope with images of different cell types, multiple cells with differing morphologies and, for time-lapse data, changes in cell number and morphology (Dimopoulos et al., 2014; Meijering, 2012). However, in reality, algorithms tend to cope best with the images for which they were designed (Masuzzo et al., 2016). Thus, without exception, segmentation of both QPI and PC images requires careful selection of algorithms and optimisation of parameters at each step. The high contrast nature of QPI compared to PC images enables the former to perform with fewer steps and constraints in order to achieve accurate segmentation, which permits handling of a wider range of cell analysis problems. Historically, the cell imaging field has required new solutions for each cell analysis problem (Meijering, 2012), prompting development of new analysis tools for diverse image types (Dimopoulos et al., 2014; Hilsenbeck et al., 2016). Nevertheless, there is also a responsibility during experimental design to select an image acquisition system capable of producing high-contrast data, from which analysis tools have best chance of obtaining accurate numerical descriptions of cell phenotypes.

Following segmentation, the next challenge is to accurately track cells. Whilst manual tracking is common, it is time and labour intensive, can suffer from inter-operator variability and bias, ill-defined cell centroid positioning (Cordelieres et al., 2013), miscalculation in migration rates (Huth et al., 2010), and routines that do not co-export morphological data. Automated tracking can circumvent these issues and accurately track large numbers of cells (*e.g.* >50) more time efficiently compared to manual tracking (Cordelieres et al., 2013). Automated cell tracking algorithms can be simple, linking cells 'nearest' in position/shape/intensity etc., or more complex, *e.g.* graph-based methods (Akram et al., 2016; Winter et al., 2011). Tracked data should be carefully validated (Rapoport et al., 2011), which can be efficiently performed *via* user-interactive lineage trees (Hilsenbeck et al., 2016; Winter et al., 2011) or machine-learning methods (Lou et al., 2014). Compared to traditional techniques, the incorporation of cell intensity and morphological information extracted from QPI enables tracking algorithms to better link cells between successive frames.

4. Label-free metrics describing biological events

The label-free dynamic phenotype of every cell consists of a row of metrics (Table 1) at each time-point. Temporal readouts offer distinct advantages over fixed endpoints by enabling delineation between biological processes that show kinetic differences, *e.g.* types of cell death (Kepp et al., 2011). In the following sections, we highlight how temporal changes in different metrics can be combined to form biologically-meaningful conclusions.

4.1. Population-level metrics

Time-resolved changes in population-level metrics, such as confluency, have been used to monitor cell viability and 'growth', with particular effect in detecting subtle 'growth' changes in response to different drugs *via* PC microscopy (Blum et al., 2015; Single et al., 2015). However, confluence-based 'growth' measurements suffer from inaccuracies as they rely on 2D measurements of cell-substrate contact area, which assumes that growth only occurs as changes in cell length and width. Invariably, however, cells also alter in height during shape changes (*e.g.* rounding), thus breaking the 2D length-width assumption and rendering confluence-based 'growth' measurements inaccurate. This same assumption compromises the use of confluence as a measure of proliferation especially as 100% confluency is reached (Single et al., 2015). Consequently, more effective measurements of cell growth are preferable. As well as measuring changes in area-based cell confluence (Curl et al., 2004), QPI generates unique phase metrics, which provide accurate measurement of cell growth at an individual-cell level alongside growth and proliferation at a population level. Specifically, a cell's dry mass can be calculated from the phase delay under previously validated assumptions that the refractive increment of biomolecules can be closely approximated by a constant (Barer, 1952; Zangle and Teitell, 2014). The increase in total dry mass of cells that occurs under normal growth and proliferation can be compared to the rate of change in total dry mass observed upon treatment (Fig. 2a). Retardation or decrease in the rate of change is indicative of cytostatic or cytotoxic effects of a drug on a population and has previously yielded EC50 values that agreed with existing literature (Rappaz et al., 2014).

Population-level unique phase metrics also offer advantages over confluence measures in label-free gap closure or scratch wound assays, which measure cell migration and wound healing, respectively. Endpoint or time-lapse PC microscopy assay formats are typically used to measure the change in confluence of a cell-free region, pre-defined within a cell monolayer (Blum et al., 2015). As above, time-resolved data is preferential to fixed endpoint data as it enables detection of subtler treatment-induced changes (Jonkman et al., 2014). In all gap closure assays, potential drug-induced changes in cell proliferation must be determined and limited as appropriate by anti-proliferative treatments to prevent misinterpretation of confluence-based motility measurements. *Via* QPI, changes in the growth and proliferation rate of cells during gap closure can be monitored directly through combinatorial use of cell dry mass and thickness measurements (Bettenworth et al., 2014), negating the need for separate proliferation assays. Furthermore, PC (Bise et al., 2011) and QPI (Mov.2) can be used to automatically track individual cells within gap closure assays to reveal proliferation-independent motility measures. The following section considers the benefits and metrics of individual cell data.

4.2. Relevance of individual cell data

Cells display heterogeneous phenotypes within genetically identical populations as a result of the expression of unique transcriptomes and proteomes (Chang et al., 2008). Imaging cell populations whilst simultaneously extracting metrics from each individual cell within that population enables cell-to-cell heterogeneity to be assessed, yielding results of clinical importance *e.g.* informing strategies to overcome fractional killing of tumour cells by chemotherapeutics (Spencer et al., 2009).

4.3. Motility behaviour of individual cells

Cell motility is essential in many aspects of biology, *e.g.* immune regulation, tissue regeneration and embryogenesis. Deregulation of cell motility can result in diseases such as cancer, autoimmune disorders, neurological diseases, and chronic inflammation. Direct,

. Compared to untreated controls, 1 nM Staurosporine treatment causes emergence of subpopulations of cells with increased speed and Euclidian distance as well as decreased sphericity (*i.e.* flattening) and more directed migration. Emerging populations move outside of the red box NOT-gate over time. The bar graph indicates the percentage of cells outside of this gate for each 24 h time window.

non-invasive measurements of cell motility can be made by tracking individual cells *in vitro* using label-free imaging, with manifold benefits: (i) direct measures of cell speed, which are independent of factors such as proliferation; (ii) measures of path directionality and tortuousness; (iii) identification of cell-to-cell heterogeneity in motility. Additionally, identification of individual cells enables direct measurement of cell number; this can be underestimated by area-based confluence measures at high cell density (Single et al., 2015) or affected by treatment-induced changes in cell area. The cell numbers and [x,y] positions obtained during tracking can be used to determine the effects of cell-to-cell proximity upon migration. Numerous cell morphological metrics (Table 1) can also be considered alongside. The result is a label-free dynamic phenotype, which is rich in additional information and can be probed to extract the simplest combination of metrics unique to a given treatment.

A practical example that exploits a dynamic phenotype, which incorporates both population and individual cell metrics derived from QPI, is illustrated in Fig. 2. Here, MDA-MB-231 cells treated with 1 nM and 10 μM of Staurosporine were imaged for 72 h by ptychographic QPI. Population-level indicators of cell growth, confluence, proliferation and viability indicated that cells were only killed with 10 μM Staurosporine (Fig. 2a). However, individual cell data revealed that 1 nM Staurosporine caused a subset of cells to exhibit more directed motion, become elongated, and roam further from neighbouring cells when compared to control cells (Fig. 2b). The results suggest treatment of MDA-MB-231 cells with sub-toxic concentrations of Staurosporine elicits a pro-migratory phenotype in a subset of cells. This example data demonstrates the power of individual cell measurements for creating dynamic phenotypes to annotate the effects of drugs/treatments that are not captured by population-level approaches nor endpoint analysis.

4.4. Cell cycle and lineage

Deregulation of the cell cycle is a hallmark of cancer. Label-free imaging offers a non-invasive solution to track temporal perturbations in the cell cycle in individual cells through successive divisions (*i.e. in vitro* lineage tracing). A key step involves detection of patterns of metrics that indicate mitosis, which has been successfully achieved for both PC and QPI techniques (Huh et al., 2011; Marrison et al., 2013; Masuzzo et al., 2016; Rapoport et al., 2011; Zangle et al., 2014). Output measurements are timeframes associated with mitosis and have uses in the development of anti-mitotic cancer drugs. Label-free imaging is particularly suited to cell cycle/*in vitro* lineage tracing that necessitates long-term analysis of successive cell divisions of individual cells. Example applications include the origins of trisomies (Gisselsson et al., 2010) and restricted stem cell colony formation (Barbaric et al., 2014). Critically, label-free technologies enable these results to be obtained without adding labels that potentially alter normal cell proliferative behaviour.

Discrimination between cell cycle stages is an active area of label-free research. Recently, label-free identification of DNA content and mitotic phases was achieved *via* imaging *flow cytometry* and machine-learning (Blasi et al., 2016). For discrimination between cell cycle stages *via* label-free microscopy, QPI represents a likely candidate for success as image intensity information relates to cellular biomolecule content and structure. Although numerous label-free QPI metrics have been proposed for different cell cycle stages (Girshovitz and Shaked, 2012; Mir et al., 2011), only one study validated the cell cycle stage with correlative fluorescent markers (Mir et al., 2011). Fluorescent biosensors demark specific biochemical processes and can be useful in annotating a dynamic phenotype in order to validate label-free patterns, thus necessitating the existence of QPI systems that offer correlative fluorescence capability and allowing a ground truth to be established.

5. Future perspectives

We have illustrated that high-contrast image outputs from QPI systems produce label-free dynamic phenotypes, which can discriminate between changes in cell behaviour not captured by typical population-level approaches or endpoint assays. Yet efficient analysis of this type of data can be challenging. The sheer quantity of values recorded within a label-free dynamic phenotype necessitates increased computational time and development of analysis strategies to fully understand the data. To date, strategies such as surface-level combinatorial metric analyses have proved useful, for example in discriminating between cell types in complex culture (Suman et al., 2016); however advanced analysis strategies such as nth-dimensional parameter space and support vector machines (Feng et al., 2009) will need to be utilised to reveal novel behaviours and subpopulations of cells that are not immediately apparent in the data.

Efforts are also being made to develop label-free imaging systems compatible with 3D samples *e.g.* spheroids and organoids. Whilst implementation for QPI and PC remains at proof-of-concept stage, 3D imaging systems will enable deeper imaging of unlabelled samples as opposed to typical 2D QPI systems where imaging depth is limited to within a few tens of microns (Adanja et al., 2010; Godden et al., 2014). Realising label-free 3D imaging will help to alleviate reliance on fluorescent dyes and offer non-invasive insights into native cell behaviour within the context of 3D extracellular environments.

Funding

This work was partly supported by Innovate UK and EPSRC in the form of a Knowledge Transfer Partnership (KTP No. 009111) between Phasefocus and The University of York.

Acknowledgements

We would like to thank M.J. Humphry for advice and critical reading of the manuscript as well as J. Marrison and G. Park for technical assistance. We would also like to thank Phasefocus, UK for use of VL-21 and Livecyte systems that were used to acquire all QPI data presented in the figures.

Appendix A. Supplementary data

Supplementary data associated with this article can be found, in the online version, at http://dx.doi.org/10.1016/j.biocel.2017.01.004.

References

Adanja, I., Debeir, O., Megalizzi, V., Kiss, R., Warzee, N., Decaestecker, C., 2010. Automated tracking of unmarked cells migrating in three-dimensional matrices applied to anti-cancer drug screening. Exp. Cell. Res. 316, 181–193.

Akram, S.U., Kannala, J., Eklund, L., Heikkil, J., 2016. Joint cell segmentation and tracking using cell proposals. 2016 IEEE 13th International Symposium on Biomedical Imaging (ISBI), 920–924.

Alford, R., Simpson, H.M., Duberman, J., Hill, G.C., Ogawa, M., Regino, C., Kobayashi, H., Choyke, P.L., 2009. Toxicity of organic fluorophores used in molecular imaging: literature review. Mol. Imaging 8, 341–354.

Arce, S.H., Wu, P.H., Tseng, Y., 2013. Fast and accurate automated cell boundary determination for fluorescence microscopy. Sci. Rep. 3, 2266.

Bajcsy, P., Cardone, A., Chalfoun, J., Halter, M., Juba, D., Kociolek, M., Majurski, M., Peskin, A., Simon, C., Simon, M., Vandecreme, A., Brady, M., 2015. Survey statistics of automated segmentations applied to optical imaging of mammalian cells. BMC Bioinf. 16, 330.

Barbaric, I., Biga, V., Gokhale, P.J., Jones, M., Stavish, D., Glen, A., Coca, D., Andrews, P.W., 2014. Time-lapse analysis of human embryonic stem cells reveals multiple bottlenecks restricting colony formation and their relief upon culture adaptation. Stem Cell Rep. 3, 142–155.

Barer, R., 1952. Interference microscopy and mass determination. Nature 169, 366–367.
Bettenworth, D., Lenz, P., Krausewitz, P., Bruckner, M., Ketelhut, S., Domagk, D., Kemper, B., 2014. Quantitative stain-free and continuous multimodal monitoring of wound healing in vitro with digital holographic microscopy. PLoS One 9, e107317.
Bise, R., Kanade, T., Yin, Z., Huh, S.i., 2011. Automatic cell tracking applied to analysis of cell migration in wound healing assay. 2011 Annual International Conference of the IEEE Engineering in Medicine and Biology Society, 6174–6179.
Blasi, T., Hennig, H., Summers, H.D., Theis, F.J., Cerveira, J., Patterson, J.O., Davies, D., Filby, A., Carpenter, A.E., Rees, P., 2016. Label-free cell cycle analysis for high-throughput imaging flow cytometry. Nat. Commun. 7, 10256.
Blum, W., Pecze, L., Felley-Bosco, E., Schwaller, B., 2015. Overexpression or absence of calretinin in mouse primary mesothelial cells inversely affects proliferation and cell migration. Respir. Res. 16, 153.
Carlton, P.M., Boulanger, J., Kervrann, C., Sibarita, J.B., Salamero, J., Gordon-Messer, S., Bressan, D., Haber, J.E., Haase, S., Shao, L., Winoto, L., Matsuda, A., Kner, P., Uzawa, S., Gustafsson, M., Kam, Z., Agard, D.A., Sedat, J.W., 2010. Fast live simultaneous multiwavelength four-dimensional optical microscopy. Proc. Natl. Acad. Sci. U. S. A. 107, 16016–16022.
Chang, H.H., Hemberg, M., Barahona, M., Ingber, D.E., Huang, S., 2008. Transcriptome-wide noise controls lineage choice in mammalian progenitor cells. Nature 453, 544–547.
Cordelieres, F.P., Petit, V., Kumasaka, M., Debeir, O., Letort, V., Gallagher, S.J., Larue, L., 2013. Automated cell tracking and analysis in phase-contrast videos (iTrack4U): development of Java software based on combined mean-shift processes. PLoS One 8, e81266.
Coutu, D.L., Schroeder, T., 2013. Probing cellular processes by long-term live imaging–historic problems and current solutions. J. Cell. Sci. 126, 3805–3815.
Curl, C.L., Harris, T., Harris, P.J., Allman, B.E., Bellair, C.J., Stewart, A.G., Delbridge, L.M., 2004. Quantitative phase microscopy: a new tool for measurement of cell culture growth and confluency in situ. Pflugers Arch. 448, 462–468.
Dimopoulos, S., Mayer, C.E., Rudolf, F., Stelling, J., 2014. Accurate cell segmentation in microscopy images using membrane patterns. Bioinformatics 30, 2644–2651.
Feng, Y., Mitchison, T.J., Bender, A., Young, D.W., Tallarico, J.A., 2009. Multi-parameter phenotypic profiling: using cellular effects to characterize small-molecule compounds. Nat. Rev. Drug Discov. 8, 567–578.
Girshovitz, P., Shaked, N.T., 2012. Generalized cell morphological parameters based on interferometric phase microscopy and their application to cell life cycle characterization. Biomed. Opt. Express. 3, 1757–1773.
Gisselsson, D., Jin, Y., Lindgren, D., Persson, J., Gisselsson, L., Hanks, S., Sehic, D., Mengelbier, L.H., Ora, I., Rahman, N., Mertens, F., Mitelman, F., Mandahl, N., 2010. Generation of trisomies in cancer cells by multipolar mitosis and incomplete cytokinesis. Proc. Natl. Acad. Sci. U. S. A. 107, 20489–20493.
Godden, T.M., Suman, R., Humphry, M.J., Rodenburg, J.M., Maiden, A.M., 2014. Ptychographic microscope for three-dimensional imaging. Opt. Express. 22, 12513–12523.
Hilsenbeck, O., Schwarzfischer, M., Skylaki, S., Schauberger, B., Hoppe, P.S., Loeffler, D., Kokkaliaris, K.D., Hastreiter, S., Skylaki, E., Filipczyk, A., Strasser, M., Buggenthin, F., Feigelman, J.S., Krumsiek, J., van den Berg, A.J., Endele, M., Etzrodt, M., Marr, C., Theis, F.J., Schroeder, T., 2016. Software tools for single-cell tracking and quantification of cellular and molecular properties. Nat. Biotechnol. 34, 703–706.
Huh, S., Ker, D.F., Bise, R., Chen, M., Kanade, T., 2011. Automated mitosis detection of stem cell populations in phase-contrast microscopy images. IEEE Trans. Med. Imaging 30, 586–596.
Huth, J., Buchholz, M., Kraus, J.M., Schmucker, M., von Wichert, G., Krndija, D., Seufferlein, T., Gress, T.M., Kestler, H.A., 2010. Significantly improved precision of cell migration analysis in time-lapse video microscopy through use of a fully automated tracking system. BMC Cell Biol. 11, 1–12.
Jonkman, J.E., Cathcart, J.A., Xu, F., Bartolini, M.E., Amon, J.E., Stevens, K.M., Colarusso, P., 2014. An introduction to the wound healing assay using live-cell microscopy. Cell Adhes. Migr. 8, 440–451.
Kepp, O., Galluzzi, L., Lipinski, M., Yuan, J., Kroemer, G., 2011. Cell death assays for drug discovery. Nat. Rev. Drug Discov. 10, 221–237.
Lou, X., Schiegg, M., Hamprecht, F.A., 2014. Active structured learning for cell tracking: algorithm, framework, and usability. IEEE Trans. Med. Imaging 33, 849–860.
Magidson, V., Khodjakov, A., 2013. Circumventing photodamage in live-cell microscopy. Methods Cell. Biol. 114, 545–560.
Marrison, J., Raty, L., Marriott, P., O'Toole, P., 2013. Ptychography-a label free, high-contrast imaging technique for live cells using quantitative phase information. Sci. Rep. 3, 2369.
Maska, M., Danek, O., Garasa, S., Rouzaut, A., Munoz-Barrutia, A., Ortiz-de-Solorzano, C., 2013. Segmentation and shape tracking of whole fluorescent cells based on the Chan-Vese model. IEEE Trans. Med. Imaging 32, 995–1006.
Masuzzo, P., Van Troys, M., Ampe, C., Martens, L., 2016. Taking aim at moving targets in computational cell migration. Trends Cell Biol. 26, 88–110.
Meijering, E., 2012. Cell segmentation: 50 years down the road. IEEE Signal Process Mag. 29, 140–145.
Mir, M., Wang, Z., Shen, Z., Bednarz, M., Bashir, R., Golding, I., Prasanth, S.G., Popescu, G., 2011. Optical measurement of cycle-dependent cell growth. Proc. Natl. Acad. Sci. U. S. A. 108, 13124–13129.
Nketia, T.A., Rittscher, J., Noble, A.J., 2014. Utilizing phase retardation features for segmenting cells in phase contrast microscopy images, Medical Image Understanding and Analysis. In: 18th Annual Conference, MIUA 2014, Royal Holloway, UK, July 2014, Proceedings.
Rapoport, D.H., Becker, T., Madany Mamlouk, A., Schicktanz, S., Kruse, C., 2011. A novel validation algorithm allows for automated cell tracking and the extraction of biologically meaningful parameters. PLoS One 6, e27315.
Rappaz, B., Breton, B., Shaffer, E., Turcatti, G., 2014. Digital holographic microscopy: a quantitative label-free microscopy technique for phenotypic screening. Comb. Chem. High Throughput Screen 17, 80–88.
Saetzler, R.K., Jallo, J., Lehr, H.A., Philips, C.M., Vasthare, U., Arfors, K.E., Tuma, R.F., 1997. Intravital fluorescence microscopy: impact of light-induced phototoxicity on adhesion of fluorescently labeled leukocytes. J. Histochem. Cytochem. 45, 505–513.
Single, A., Beetham, H., Telford, B.J., Guilford, P., Chen, A., 2015. A comparison of real-time and endpoint cell viability assays for improved synthetic lethal drug validation. J. Biomol. Screen. 20, 1286–1293.
Spencer, S.L., Gaudet, S., Albeck, J.G., Burke, J.M., Sorger, P.K., 2009. Non-genetic origins of cell-to-cell variability in TRAIL-induced apoptosis. Nature 459, 428–432.
Suman, R., Smith, G., Hazel, K.E., Kasprowicz, R., Coles, M., O'Toole, P., Chawla, S., 2016. Label-free imaging to study phenotypic behavioural traits of cells in complex co-cultures. Sci. Rep. 6, 22032.
Tinevez, J.Y., Dragavon, J., Baba-Aissa, L., Roux, P., Perret, E., Canivet, A., Galy, V., Shorte, S., 2012. A quantitative method for measuring phototoxicity of a live cell imaging microscope. Methods Enzymol. 506, 291–309.
Wiesmann, V., Franz, D., Held, C., Munzenmayer, C., Palmisano, R., Wittenberg, T., 2015. Review of free software tools for image analysis of fluorescence cell micrographs. J. Microsc. 257, 39–53.
Winter, M., Wait, E., Roysam, B., Goderie, S.K., Ali, R.A., Kokovay, E., Temple, S., Cohen, A.R., 2011. Vertebrate neural stem cell segmentation, tracking and lineaging with validation and editing. Nat. Protoc. 6, 1942–1952.
Zangle, T.A., Teitell, M.A., 2014. Live-cell mass profiling: an emerging approach in quantitative biophysics. Nat. Methods 11, 1221–1228.
Zangle, T.A., Teitell, M.A., Reed, J., 2014. Live cell interferometry quantifies dynamics of biomass partitioning during cytokinesis. PLoS One 9, e115726.